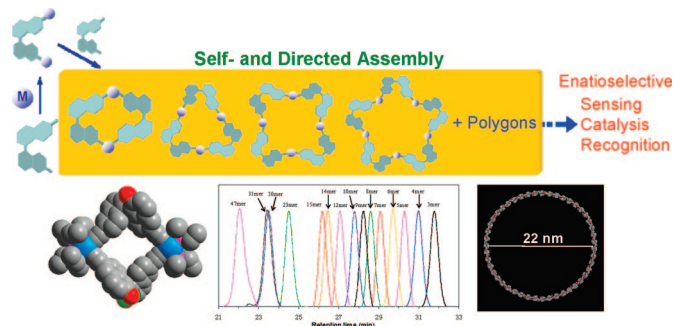# Chiral Metallocycles: Rational Synthesis and Novel Applications

SUK JOONG LEE AND WENBIN LIN*

Department of Chemistry, CB#3290, University of North Carolina,
Chapel Hill, North Carolina 27599

CONSPECTUS

Chiral supramolecular systems have attracted a great deal of interest from synthetic chemists over the past two decades because of their ability to mimic complex biological processes and their potential applications in enantioselective events such as asymmetric catalysis and chiral sensing. Chiral metallocycles, among the simplest forms of chiral supramolecular systems, are of particular interest because of their relative ease of synthesis. In this Account, we survey recent developments in the rational design and synthesis of chiral metallocyclic systems based on metal–ligand coordination and their potential applications in enantioselective recognition and catalysis.

General design principles for metallocycles are first introduced with particular focus on thermodynamic and kinetic considerations. The symmetry requirements for the linear and angular building units, the influence of stoichiometries and reaction concentrations, and the roles of solvents are discussed. Optimum synthetic conditions for the self-assembly and directed-assembly of metallocycles are also compared.

Three synthetic strategies for chiral metallocycles are broadly categorized based on the source of chirality, namely, (1) introduction of metallocorners containing chiral capping groups, (2) use of metal-based chirality owing to specific coordination arrangements, and (3) introduction of chiral bridging ligands. The bulk of this Account focuses on the third synthetic strategy with examples of chiral metallocycles built from atropisomeric bridging ligands based on the 1,1′-binaphthalene framework. The influences of ligand geometries and metallocorner configurations on the metallocycle structures are demonstrated. The synthetic utility of directed-assembly processes is illustrated with numerous examples of cyclic polygons ranging from nanoscopic dimers to a mesoscopic 47mer. Moreover, the directed-assembly processes offer exquisite control on structure, chirality, and functionality of the metallocycles.

A number of interesting applications have been demonstrated with chiral metallocycles with diverse sizes and functionalities. For example, metallocycles with the Pt(diimine) metallocorners show interesting behaviors as luminophores in prototype light-emitting devices, chiral molecular squares based on 1,1′-binaphthyl-derived bipyridyl bridging ligands and fac-Re(CO)$_3$Cl corners exhibit enantioselective luminescence in the presence of the 2-amino-1-propanol analyte, and chiral metallocycles based on 1,1′-binaphthyl-derived bialkynyl bridging ligands and cis-Pt(PEt)$_2$ corners activate Ti(IV) centers to catalyze highly enantioselective diethylzinc additions to aromatic aldehydes to afford chiral secondary alcohols. Additionally, chiral metallocycles synthesized via the weak-link approach (WLA) are shown to exhibit allosteric regulation. They experience significant changes in the cavity sizes and shapes upon the introduction of other ligands, with the resulting open structures serving as a catalyst for acyl transfer reaction or as an enantioselective recognition pocket.

In summary, chiral metallocycles with much enhanced stability, favorable solubility characteristics, unprecedentedly large sizes, well-positioned functional groups, and desired chirality have been synthesized using a combination of self- and directed-assembly strategies. The applications of these chiral metallocycles in light-emitting devices, allosteric regulation, chiral sensing, and asymmetric catalysis have been demonstrated. The examples illustrated in this Account give testimony to chemists' ability, through chemical manipulations, to create large and complex chiral metallocycles that can potentially serve as mimics of natural enzyme systems.

Introduction

One of the most important goals in modern supramolecular chemistry is to develop efficient synthetic strategies for large molecular architectures that reach the hierarchical complexity of natural systems. Such biomimetic synthetic models should facilitate fundamental studies of Nature's highly efficient biochemical machineries and are a key focus of current molecular nanotechnology.[1,2] Stepwise synthetic procedures are the most widely used routes to constructing a variety of compounds. These methods are extremely powerful for the synthesis of small organic molecules, but often time- and yield-prohibitive for large molecules, especially those that approach Nature's complexity. Much effort has therefore been directed toward developing alternative synthetic strategies for large supramolecular structures such as macrocycles and cages.[3,4]

Self-assembly synthetic schemes have been shown to be extremely useful for highly symmetrical large molecular architectures. Properly designed and preprogrammed building units can spontaneously assemble into well-defined and thermodynamically stable supramolecular products.[5] Such a self-assembly process takes advantage of kinetically labile bonds between building units to eliminate potential defects that might lead to product heterogeneity. Under proper synthetic conditions, the assemblage can undergo self-sorting[6] and self-correcting processes until all the components congregate into well-defined final products that are the most stable thermodynamically.[7] The synthesis of phenol–formaldehyde or resorcinol–aldehyde cyclic oligomers, known as calixarenes, is a good example of high-yield macrocycle formation under such a thermodynamic control.[8] The self-sorting and self-correcting ability of well-defined supramolecular architectures is driven by noncovalent bonds such as hydrophobic/hydrophilic considerations, $\pi-\pi$ interactions, hydrogen bonding, and metal–ligand coordination.[9,10] In particular, metal–ligand coordination chemistry has been used extensively to construct supramolecular structures such as helices,[11] tubes,[12] metallocycles, and cages.[13,14] These architectures are spontaneously generated by simply mixing component building units (ligands and metallocorners) in solution. Rich coordination chemistry has been used to construct a wide variety of metallocycles by incorporating the binding sites with suitable angles.[1,5] In this Account, we will review recent developments on the rational synthesis and applications of a subclass of metal-containing macrocycles, namely, chiral metallocycles.

Design Principles for Metallocycles

The symmetry of individual building units and the overall shape of the resulting assembly are the most important factors to be cogitated in the rational design of discrete metallocycles. Milestone works by Fujita[1,2] and Stang[5,7,15] have clearly demonstrated the ability to efficiently construct small molecular polygons based on metal–ligand coordination with appropriate rigid and directional building units. These pioneering examples have shown that two types of building units (linear and angular) are required to construct molecular polygons with a high efficiency. Linear building units possess two active functional end groups that are oriented 180° from each other and can only interact with the end groups of angular building units. The final shapes and symmetries of the resulting assemblies will solely depend on the type and stoichiometry of linear and angular building units. A remarkably large variety of metallocycles has been constructed via self-assembly of angular and linear building units, and their structures can be readily rationalized based on such simple symmetry and geometric considerations. For example, the assembly of a planar triangle can be achieved by combining three linear building subunits and three 60° angular ones. A molecular square can be constructed in several different ways, including a combination of four linear and four 90° angular building units and a combination of two different 90° angular building units. Combining five linear subunits with five angular ones that possess a 108° angle between their binding sites will generate a molecular pentagon (Figure 1). These predictions of metallocycle sizes assume total conformational rigidity of subunits, but deviations from the ideal binding angles can occur. Metallocycles of different shapes from those predicted by these simple geometrical considerations can occasionally result because of conformational flexibility of the building units.
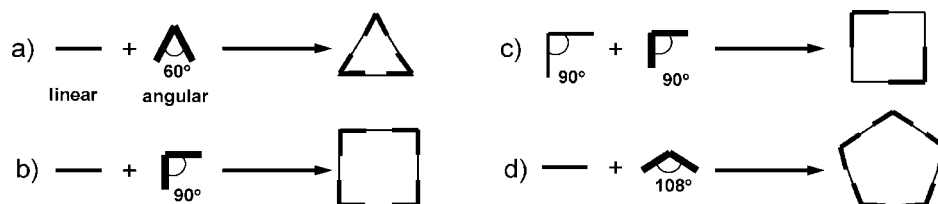

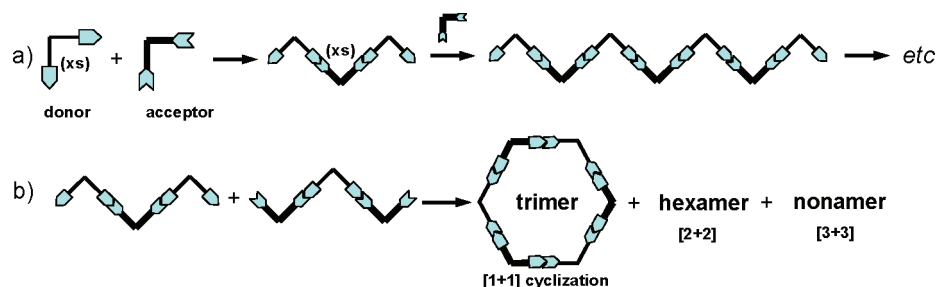**FIGURE 1.** Schematic representation of the self-assembly of simple metallocycles.

FIGURE 2. Schematic representation for directed assembly of large kinetically controlled metallocycles.

Thermodynamic and Kinetic Considerations

Most of the known metallocycles were obtained via spontaneous self-assembly of properly chosen building blocks.[5] The key to successful self-assembly reactions is that the entire assembly must be able to undergo self-correcting processes to access the thermodynamically stable species.[16,17] Three critical conditions need to be considered for the synthesis of metallocycles under thermodynamic control: (i) the bonds must form only between the building units' active functional end groups, (ii) the bonds must be kinetically labile to allow for self-correction, and (iii) the resulting species must be thermodynamically favored over competing species.[9]

It is well-established that closed cyclic structures are enthalpically favored over open ones because a larger number of metal–ligand bonds are formed than in open oligomeric species. Although acyclic oligomers may polymerize to increase the number of bonds formed, the donor and acceptor sites at each end of the polymer will always remain uncoordinated. When cyclization is unfavorable, the oligomers will likely polymerize until higher oligomers precipitate as kinetic products.

Small metallocycles are favored over larger ones for entropic reasons. Assuming negligible steric effects and ring strain, the free energy change of the macrocyclic equilibrium is $\Delta G = -T\Delta S$, which indicates that the equilibrium is dominated by the entropy of the system. As the equilibrium shifts from smaller to larger cyclic assemblies, the smaller population of large cycles leads to a decrease of the entropy ($\Delta S < 0$) and thus an increase of the free energy ($\Delta G > 0$). The equilibrium shift from smaller cycles to larger cycles is thus disfavored, and smaller cycles often represent the lowest energy structure. As a result, many molecular triangles and squares are reported in the literature, and very few large metallocycles are known.[18,19]

Solvents often play an important role in the self-assembly of metallocycles. The high yields of these thermodynamically controlled processes are a consequence of kinetic lability of the metal–ligand bonds. The ability to self-correct to reach the most stable structure is often facilitated by the use of appropriate solvents. The solvent molecule can act as a weakly coordinating ligand and assists to solubilize various fragments and open-chain oligomers yet can be readily displaced by the bridging ligand for cycle formation.[20]

Much larger metallocycles can on the other hand be obtained in a kinetically controlled reaction that is typically carried out under high dilution conditions.[21] In such cases, the self-correction process is not operative and well-defined building blocks with appropriate geometrical features are even more important for predictable synthesis of kinetically controlled macrocycles. The formation of different sizes of linear intermediates makes it possible to form larger cycles during the reaction. Smaller cycles will still be favored over larger cycles in such kinetically controlled reactions owing to kinetic factors.

The preference for forming smaller metallocycles during kinetically controlled syntheses can be overcome by using the so-called directed-assembly strategy. As shown schematically in Figure 2, ligand-terminated acyclic oligomers can be synthesized by using a large excess of the ligand relative to the metal connecting unit via an iterative stepwise growth process. Under optimal conditions, the ligand-terminated acyclic oligomers can be purified by chromatography or crystallization. Metal-terminated acyclic oligomers can be synthesized using the same strategy. Combination of both ligand- and metal-terminated acyclic oligomers in a 1:1 molar ratio will lead to much larger metallocycles than those possible from the self-assembly of simple ligand and metal connecting units. In such directed-assembly processes, metallocycles can only result from [1 + 1], [2 + 2], [3 + 3], or higher-order cyclization reactions. Our recent work has shown that metallocycles of unprecedentedly large sizes can be synthesized using this directed-assembly strategy.[21]

Synthetic Strategies toward Chiral Metallocycles

Owing to the importance of chirality in biological processes, there is a keen need for the ability to efficiently synthesize
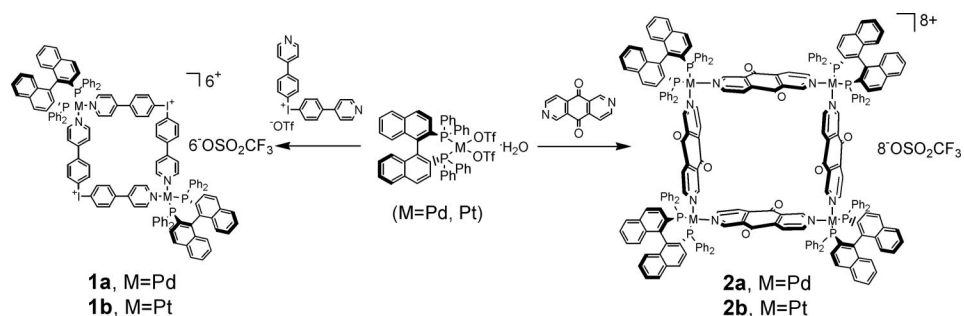
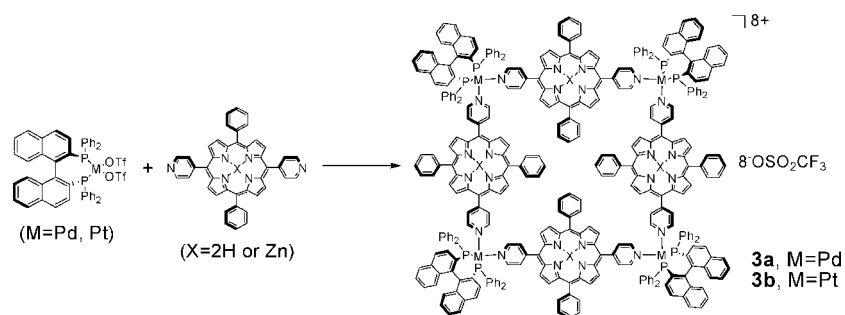**FIGURE 3.** Synthesis of chiral metallocycles with chiral metallocorners.

FIGURE 4. Porphyrin-containing chiral metallocycles.

chiral molecules.[22] Chiral supramolecular systems have attracted a great deal of interest from synthetic chemists because of their potential utility in enantioselective events such as sensing and asymmetric catalysis over the past two decades.[23] Although numerous metallocycles have been reported, few of them were designed with such a functional consideration. Chiral metallocycles are thus an interesting synthetic target owing to the prospect that well-designed chiral metallocycles can possess enzyme-like chiral pockets and functionalities for applications in chiral sensing and asymmetric catalysis.[24]

Three distinct strategies have been employed for the construction of chiral metallocycles: (1) introduction of chiral metallocorners that possess chiral capping groups, (2) use of metal-based chirality owing to specific coordination arrangements, and (3) introduction of chiral bridging ligands. In the first approach, chiral metallocycles were prepared by the interaction between achiral bridging ligands and metallocorners with chiral chelating groups. Optically active metal complexes with [M(R-BINAP)(OTf)$_2$] (M = Pd or Pt, BINAP = 2,2'-bis(diphenylphosphino)-1,1'-binaphthalene) as a chiral building block have been used to construct chiral molecular squares (Figure 3).[25] When combined with bis(4-(4'-pyridyl)phenyl)iodonium triflate, heteronuclear optically active cyclic species **1a** and **1b** were obtained. These molecular squares are chiral due only to the chiral transition-metal auxiliary (BINAP) in the assembly. Both **1a** and **1b** possess D_2 symmetry, with one C_2 axis

passing through the center of the binaphthyl rings and the other C_2 axis passing through the two iodine atoms.

Chiral tetranuclear molecular squares[25] were readily synthesized when [M(R-BINAP)(OTf)$_2$] was treated with C_{2h}-symmetrical diaza ligands 2,6-diazaanthracene (DAA) in acetone. Only a single diastereomer was obtained as evidenced by a single signal in the ^{31}P NMR spectrum. In contrast, when 2,6-diazaanthracene-9,10-dione (DAAD) was used in place of DAA (Figure 3), the reaction mixture consisted of a dominant diastereomer of **2a** and **2b** in a diastereomeric excess (de) of 81% and minor amounts of other diastereomers. These chiral molecular squares were also characterized by electrospray mass spectrometry (ESI-MS). Stang et al. also synthesized a family of interesting chiral molecular squares containing porphyrins by using *trans*-5,15-di(4'-pyridyl)porphyrin (*trans*-DPy-DPP) as the linear modules and enantiopure BINAP-Pd(II) as the angular units (Figure 4).[26] The rotation of the metal–pyridyl bonds in **3** is restricted at room temperature, and the chirality of the metallocorners thus promotes the formation of enantiomeric macrocycles with a puckered geometry.

In the second strategy, chiral metallocycles were assembled by exploiting the coordination geometries of octahedral transition metal complexes. Zhang and co-workers[27] reported the assembly of chiral molecular squares using achiral building blocks. When two achiral bidentate ligands interact with octahedral metal ions such as Co(II) or Mn(II), the resulting octahedral complexes become chiral. No chiral auxiliary
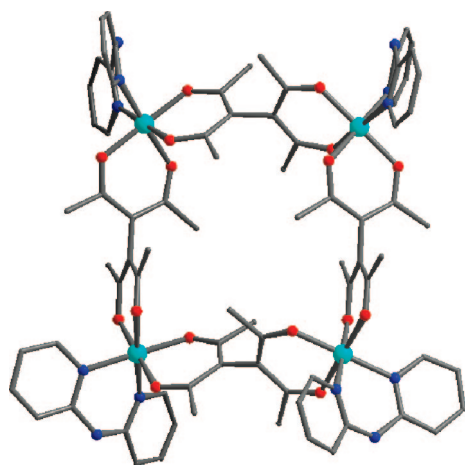
FIGURE 5. Single-crystal X-ray structure of $Co_4(tae)_4(dpa)_4$, **4**.

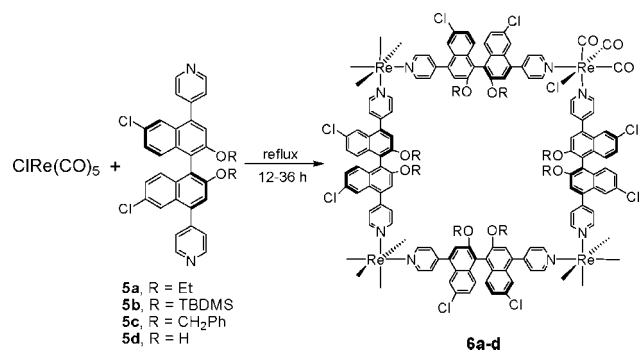**FIGURE 6.** Synthesis of chiral molecular squares based on enantiopure linear 1,1'-binaphthyl-derived bipyridyl bridging ligands and *fac*-$Re(CO)_3Cl$ corners.
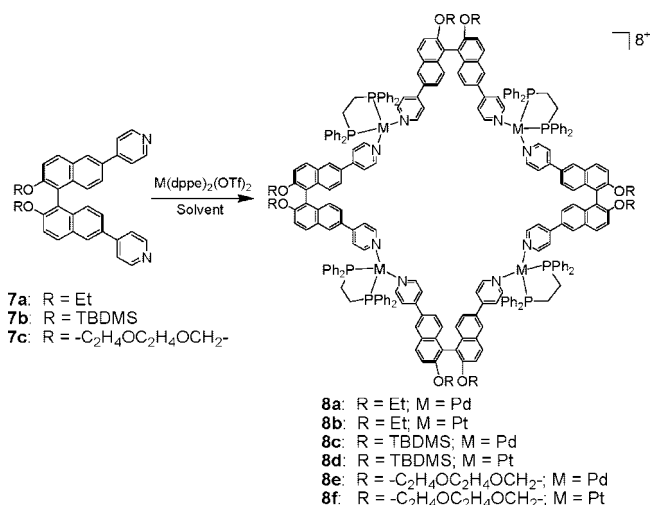

FIGURE 7. Synthesis of chiral molecular squares based on enantiopure angular 1,1'-binaphthyl-derived bipyridyl bridging ligands and $[M(dppe)]^{2+}$ metallocorners.

ligands are needed for the construction of chiral molecular squares using this strategy. For example, chiral metallocycles were obtained when the bridging ligands possessing D_{2d} symmetry, tetraacetylethylene dianion (tae), were coordinated to octahedral Co(II) metallocorners that were capped with a chelating di-2-pyridylamine (dpa) ligand. The D_{2d} symmetry is reduced to pure rotational symmetries, and chiral molecular square $Co^{II}_4(tae)_4(dpa)_4$, **4**, was obtained in 15% yield and characterized by single-crystal X-ray crystallography (Figure 5). The synthesis of **4** demonstrates that ligands with a ~90° twist between the binding sites can facilitate the formation of chiral molecular squares when octahedral metal ions are employed. Along the same line, MacDonnell et al. synthesized chiral molecular hexagons by using octahedral complexes with propeller-like arrangements of three chelating ligands around a metal center. Chiral building blocks [(bpy)Ru-(tpphz)$_2$]$^{2+}$ and [(bpy)Os(tpphz)$_2$]$^{2+}$ (where tpphz is tetrapyrido[3,2-*a*:2',3'-*c*:3'',2'''-*h*:2''',3'''-*j*]phenazine) were connected with palladium metal centers to afford hexagonal molecules with cavities as large as 5.5 nm in diameter.[28]

The third approach takes advantage of chiral bridging ligands, which contain inherent chirality. Chiral bridging ligands can be simply linked with achiral metallocorners to generate chiral metallocycles. Although this approach requires greater synthetic manipulations to prepare chiral bridging ligands, it provides a variety of possibilities to modify the resulting chiral pockets, which may contain functionalities for important applications. This approach was first used for the assembly of a family of novel chiral molecular squares by using enantiopure linear 1,1'-binaphthyl-derived bipyridyl bridging ligands **5a−d** and *fac*-$Re(CO)_3Cl$ corners (Figure 6).[29] During the assembly process, one single enantiomer was obtained in high yield, which possesses an approximate D_4

symmetry when the isomers due to the positions of Cl are ignored. The IR spectra of metallocycles **6a−d** exhibit three carbonyl stretches, consistent with the formation of the *fac*-[Cl(CO)$_3$Re] metallocorners that have local C_s symmetry.

When enantiopure angular 1,1'-binaphthyl-derived bipyridine bridging ligands and $[M(dppe)]^{2+}$ metallocorners (M = Pd or Pt) were employed, chiral molecular squares were assembled with D_4 symmetry (Figure 7).[30] The formation of chiral metallocycles was confirmed by a variety of analytical techniques including IR, UV−vis, circular dichroism (CD), NMR spectroscopy, and ESI mass spectrometry. All these chiral metallocycles are highly luminescent in solution at room temperature with quantum efficiencies of 0.06−0.63. Interestingly, a new *meso* dimeric metallocycle with C_2 symmetry is generated when equal molar enantiopure molecular squares of opposite handedness are mixed in solution due to self-discrimination and labile M−pyridyl bonds.
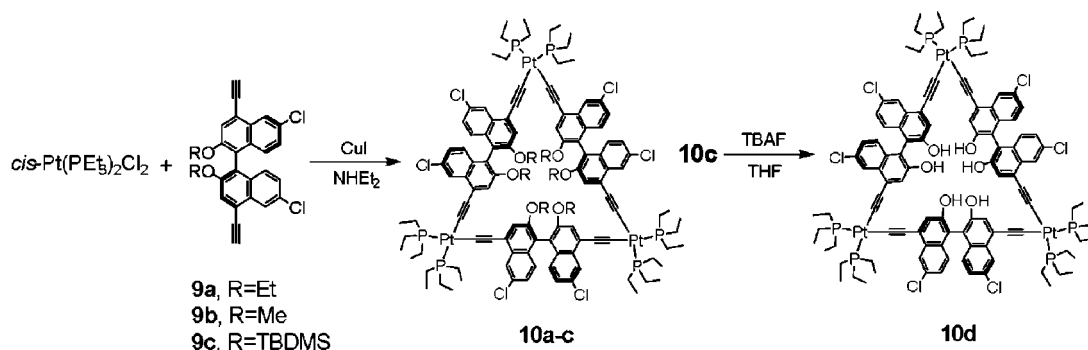
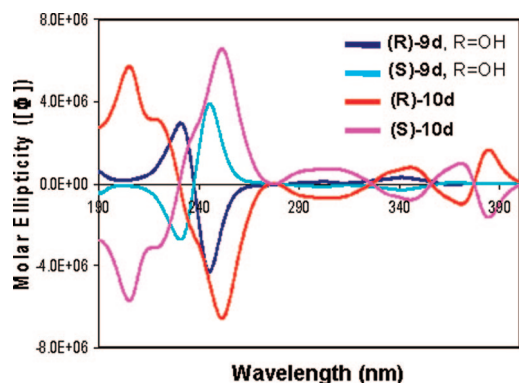**FIGURE 8.** Synthesis of chiral molecular triangles with the Pt–alkynyl linkage.

FIGURE 9. CD spectra of **9d** and **10d** in acetonitrile.

Self- and Directed-Assembly of Chiral Pt–Alkynyl Metallocycles

Due to the high stability of Pt–alkynyl bonds, many metallocyles have been constructed using the Pt–alkynyl linkage. Chiral metallocycles need to be reasonably stable for applications in many purported enantioselective events. For example, high stability and favorable solubility in nonpolar solvents are prerequisites for chiral metallocycles to be applicable in asymmetric catalytic reactions.

By taking advantage of the robust Pt–alkynyl linkage, chiral metallocycles were constructed by both self- and directed-assembly routes. As shown in Figure 8, reactions of ligands **9a–c** with equal molar equivalents of *cis*-PtCl$_2$(PEt$_3$)$_2$ in the presence of a CuI catalyst at room temperature generated chiral molecular triangles **10a–c** exclusively in modest yields.[31] Compounds **10a–d** were characterized by ^{1}H{^{31}P}, ^{13}C{^{1}H}, and ^{31}P{^{1}H} NMR spectroscopy, mass spectrometry, elemental analysis, and IR, UV–vis, and circular dichroism (CD) spectroscopies. Interestingly, CD spectra of **10a–d** exhibit an intense band at ∼202 nm, in addition to three lower-energy bands corresponding to naphthyl $\pi \rightarrow \pi^*$ transitions (Figure 9). The new CD band at ∼202 nm can be assigned to the transitions associated with *cis*-Pt(PEt$_3$)$_2$ moieties. This result suggests that the triethylphosphines on the Pt centers adopt a propeller-type arrangement (relative to the naphthyl groups), apparently steered by chiral binaphthyl moieties. Cycles **10a–d** exhibit enhanced lower-energy CD signals over the free ligands, consistent with the presence of multiple ligands in each metallocycle.

Molecular triangles were obtained from the interaction between linear ligands **9a,b,d** and the *cis*-PtCl$_2$(PEt$_3$)$_2$ metallocorners owing to their entropic advantage, although molecular squares were the expected products based on geometrical considerations. This result illustrates the kinetic preference of smaller metallocycles over the thermodynamically stable larger ones. However, this preference to form exclusively molecular triangles can be reverted to produce molecular squares based on the same building blocks via stepwise directed-assembly processes (Figure 10).[32] When the monoprotected enantiopure bis(alkynyl) **11a,b,d** was treated with 0.5 equiv of *cis*-PtCl$_2$(PEt$_3$)$_2$ in the presence of CuCl catalyst in diethylamine at room temperature, the Pt-containing intermediates **12a,b,d**, were obtained in relatively high yield (74–89%), which were further deprotected by K$_2$CO$_3$ to afford the Pt-containing intermediates with terminal alkynes **13a,b,d**. Chiral molecular squares **14a,b,d** were prepared in 34–46% yields by treating **13a,b,d** with 1 equiv of *cis*-PtCl$_2$(PEt$_3$)$_2$ in the presence of a CuCl catalyst and diethylamine at low temperatures (0 to −20 °C). All these intermediates and chiral molecular squares were characterized by ^{1}H, ^{13}C{^{1}H}, and ^{31}P{^{1}H} NMR spectroscopy, IR spectroscopy, and FAB mass spectrometry. Interestingly, when Pt(4,4'-dtbPy)Cl$_2$ was incorporated in place of *cis*-PtCl$_2$(PEt$_3$)$_2$ with linear bridging ligand **15**, both chiral molecular triangle **16** and square **17** were synthesized in 29% and 22% yield, respectively (Figure 11).[33] Molecular squares **17** were also exclusively constructed via stepwise directed-assembly reactions in modest yields.

Chiral dinuclear metallacyclophanes **19a–c** were obtained when enantiomerically pure 6,6'-bis(alkynyl)-1,1'-binaphthalene **18a–c** were reacted with 1 equiv of *cis*-Pt(PEt$_3$)$_2$Cl$_2$ (Fig-
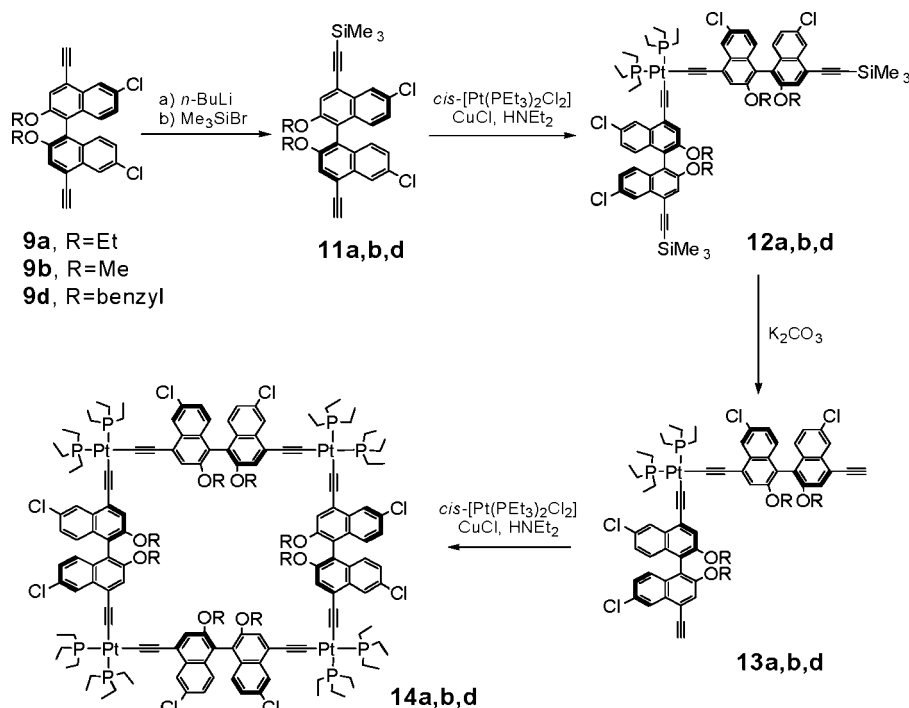
FIGURE 10. Directed synthesis of Pt−alkynyl chiral molecular squares.

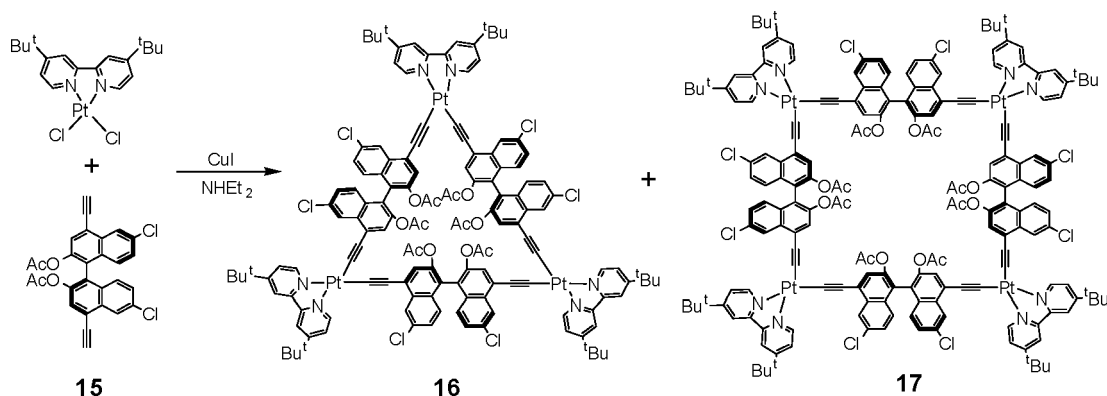**FIGURE 11.** Metallocyclic triangle and square with [Pt(4,4'-dtbPy)]$^{2+}$ metallocorners.

ure 12).[34] Single-crystal X-ray diffraction studies revealed that the two *cis*-Pt(PEt$_3$)$_2$ units were linked by two angular bis(acetylene) ligands to form a cyclic dinuclear structure **19c**. However, both Pt centers adopted slightly distorted square planar geometry with the *cis* angles around the Pt1 center ranging from 82.4(2)° to 101.3(1)° and the *cis* angles around the Pt2 center ranging from 84.3(2)° to 100.3(1)°. The rigid metallacyclophane structure of **19c** was characterized by very small dihedral angles between the naphthyl rings within each **18c** ligand (62.18° and 73.45°).

Interestingly, when topologically different 3,3'-bis(alkynyl)-1,1'-binaphthalene bridging ligands **20a−c** were used in place of their geometric isomers of **18a−c**, chiral dinuclear metallacyclophanes **21a−c** were obtained that are supramolecu-

lar isomers of **19a−c** (Figure 13).[35] Single-crystal X-ray structure determination showed that the asymmetric unit of **21c** contained two molecules of **21c** and one ethyl acetate solvent molecule. No crystallographic symmetry is present in the molecules of **21c** in the solid state. Close proximity of the 1,1'-binaphthalene units is clearly evident in the X-ray structure of **21c**, which prevents the formation of a catalytically active Ti−binolate species (see below).

Chiral molecular polygons ranging from triangle to octagon were obtained when linear *trans*-Pt(PEt$_3$)$_2$Cl$_2$ was used to connect the 6,6'-bis(alkylnyl)-1,1'-binaphthalene **18b**.[36] Each of the chiral molecular polygons [*trans*-(PEt$_3$)$_2$Pt(**18b**)]$_n$, (n = 3−8, **22−27**) was separated by silica-gel column chromatography, and analytically pure **22−27** were obtained in 5%,
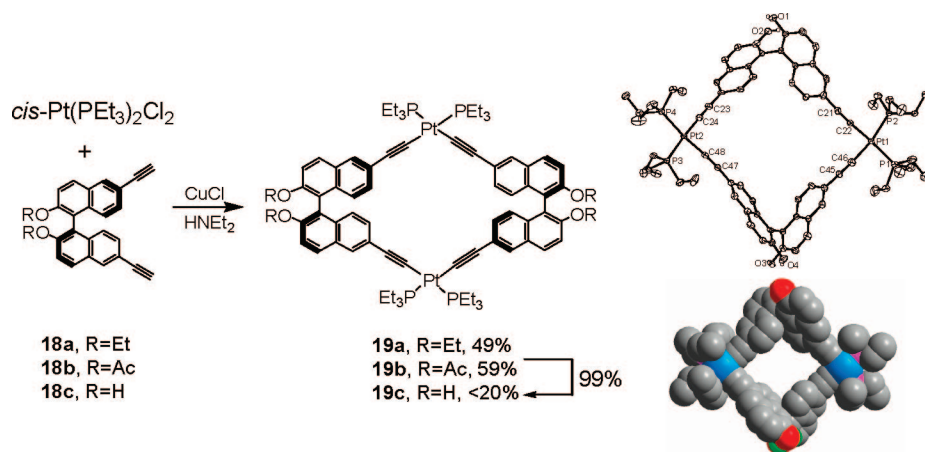
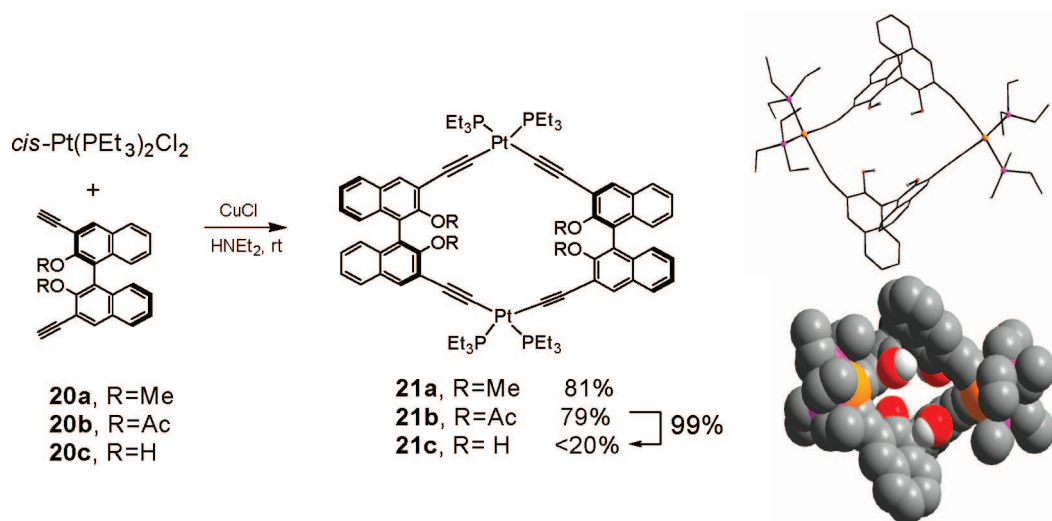**FIGURE 12.** Self-assembly of Pt−alkynyl chiral metallacyclophanes.

FIGURE 13. Self-assembly of isomeric Pt−alkynyl chiral metallacyclophanes.

18%, 16%, 10%, 5%, and 4% yield, respectively (Figure 14). Compounds **22–27** have been characterized by ^{1}H, ^{13}C{^{1}H}, and ^{31}P{^{1}H} NMR spectroscopy, FAB and MALDI-TOF MS, IR, UV−vis, and circular dichroism (CD) spectroscopies, and microanalysis. It was believed that limited conformational flexibility of the bridging ligand is a key to the facile one-pot self-assembly of chiral molecular polygons **22–27**. This result represents a rare example in which multiple products can be readily isolated from a coordination-directed self-assembly process, but still this process is not amenable to the synthesis of even larger metallocycles.

An expeditious stepwise directed-assembly strategy was developed for the synthesis of exceptionally large chiral metallocycles by cyclization of metal- and ligand-terminated oligomers.[37] These mesoscopic polygons were built from 2,2′-diacetoxy-1,1′-binaphthyl-3,3′-bis-(ethyne) bridging ligand **20b** and linear *trans*-Pt(PEt$_3$)$_2$Cl$_2$ connector. The requisite metal- and ligand-terminated oligomers were synthesized via an iter-

ative process as shown in Figure 15 and treatment of metal-terminated (**20b**)$_m$[Pt]$_{m+1}$Cl$_2$ with 1 equiv of ligand-terminated [Pt]$_n$(**20b**-2H)$_{n+1}$H$_2$ in the presence of CuCl catalyst at room temperature afforded cyclic species. For example, by treating equimolar (**20b**)[Pt]$_2$Cl$_2$ and [Pt](**20b**-2H)$_2$H$_2$, molecular triangle (25%), hexagon (45%), and nonagon (15%) were efficiently assembled with an overall yield of 85%. These chiral metallocycles were unambiguously characterized by MALDI-TOF MS and resulted from [1 + 1], [2 + 2], and [3 + 3] cyclization processes, respectively (Figure 16). Metallocycles of much larger size have been efficiently synthesized by this process (Table 1). The largest metallocycle contains 47 [Pt] and 47 **20b** units with an expected molecular weight of 39847.5 Da. Molecular mechanics simulations indicated that the internal cavities of these molecular polygons range from 0.9 to 22 nm. Size-exclusion chromatography and diffusion-order NMR spectroscopy were used to characterize these extraordinarily large chiral metallocycles. Interestingly, supramolecular iso-
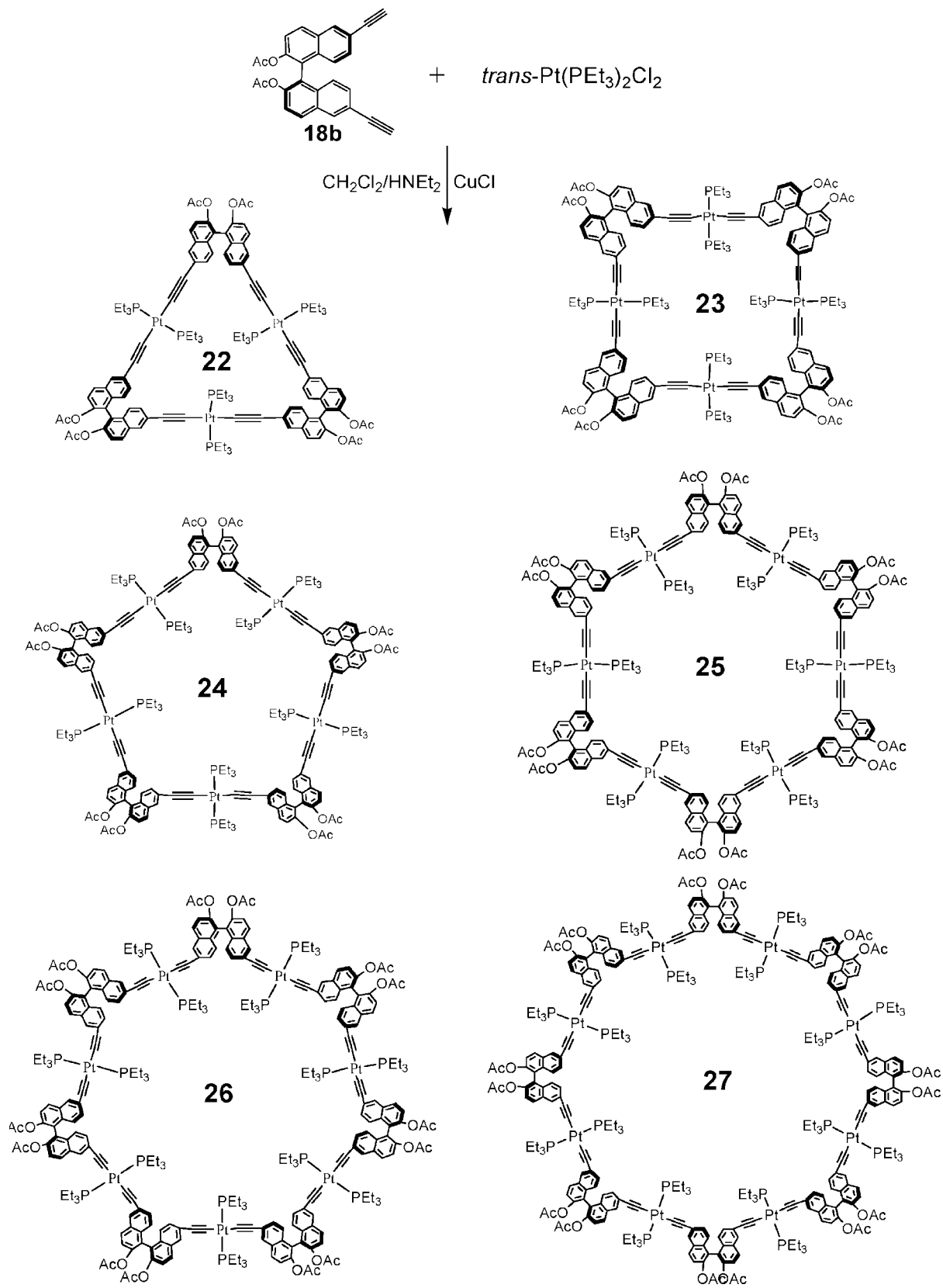
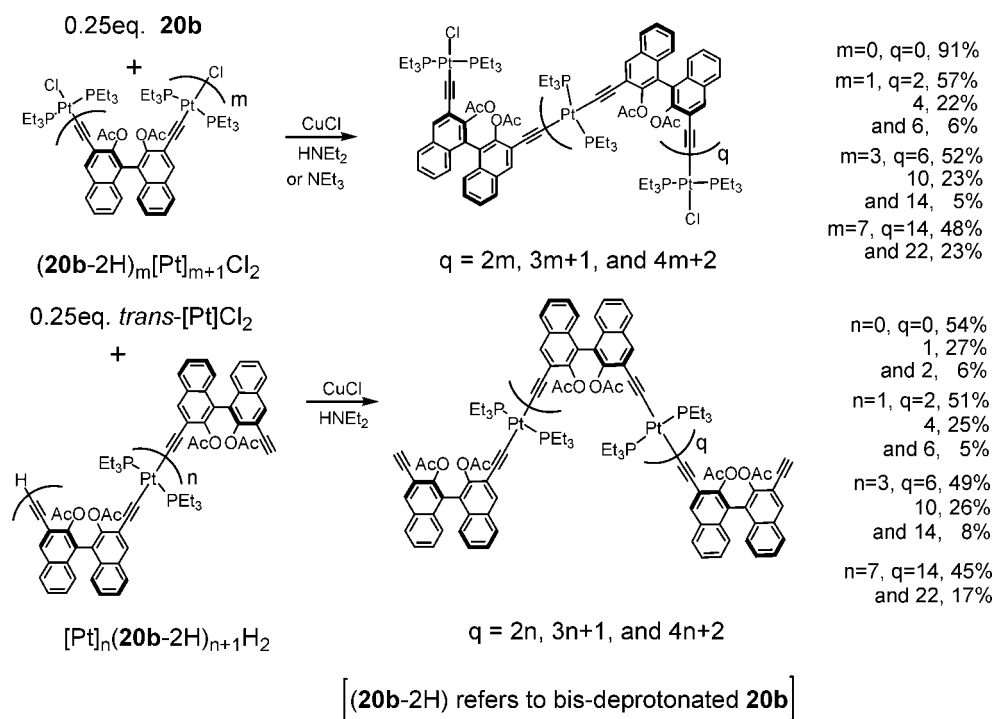**FIGURE 14.** Self-assembly of chiral molecular polygons.

FIGURE 15. Synthesis of acyclic Pt—alkynyl building blocks via directed-assembly.
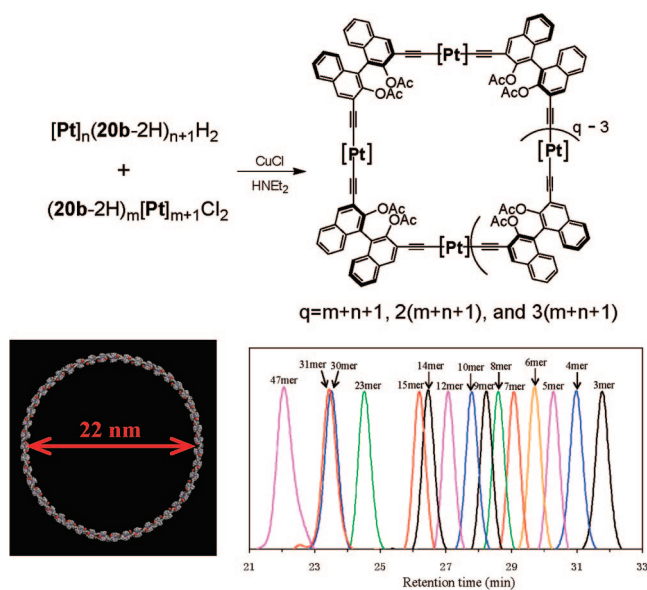

FIGURE 16. Directed-assembly of unprecedentedly large chiral metallocycles (top), energy-minimized structure of metallocycle with 47 metal centers (bottom left), and retention times of the metallocycles in SEC (bottom right).

mers of these exceptionally large metallocycles were similarly prepared when topologically different bis(alkynyl) bridging ligands **18b** were used in place of **20b**, illustrating the generality of this directed-assembly synthetic methodology.[21,38]

TABLE 1. Efficient Directed-Assembly of Exceptionally Large Chiral Metallocycles

	products (yield %)			
reagents	$(m + n + 1)$	$2(m + n + 1)$	$3(m + n + 1)$	total yield (%)
$m = 1, n = 1$	25	45	15	85
$m = 1, n = 2$	59	20	8	87
$m = 1, n = 3$	77	9	2	88
$m = 3, n = 2$	74	15		89
$m = 3, n = 3$	66	9		75
$m = 7, n = 7$	62	7		69
$m = 11, n = 11$	63			63
$m = 15, n = 15$	57			57
$m = 23, n = 23$	10			10

Directed-Assembly of Multifunctional Chiral Pt—Alkynyl Metallocycles

In addition to providing a facile route to construct extraordinarily large polygonal structures, the stepwise directed-assembly also offers exquisite control on the structure and functionality of the metallocycles. Homochiral molecular square *trans*-[(PEt$_3$)$_2$Pt]$_4$(**18b**)$_3$(**18a**), **28**, and octagon {*trans*-[(PEt$_3$)$_2$Pt]$_3$(**18b**)$_3$(**18a**)}$_2$, **29**, possessing bridging ligands with different protecting groups were prepared by treating (**18b**)$_3$[Pt]$_4$Cl$_2$ with 1 equiv of **18a** in the presence of a catalytic amount of CuCl in deaereated CH$_2$Cl$_2$ and NEt$_3$ at room temperature (Figure 17).[21] The molecular square and octagon resulted from [1 + 1] and [2 + 2] cyclization processes, respectively, and possess two types of ligands with the ratio
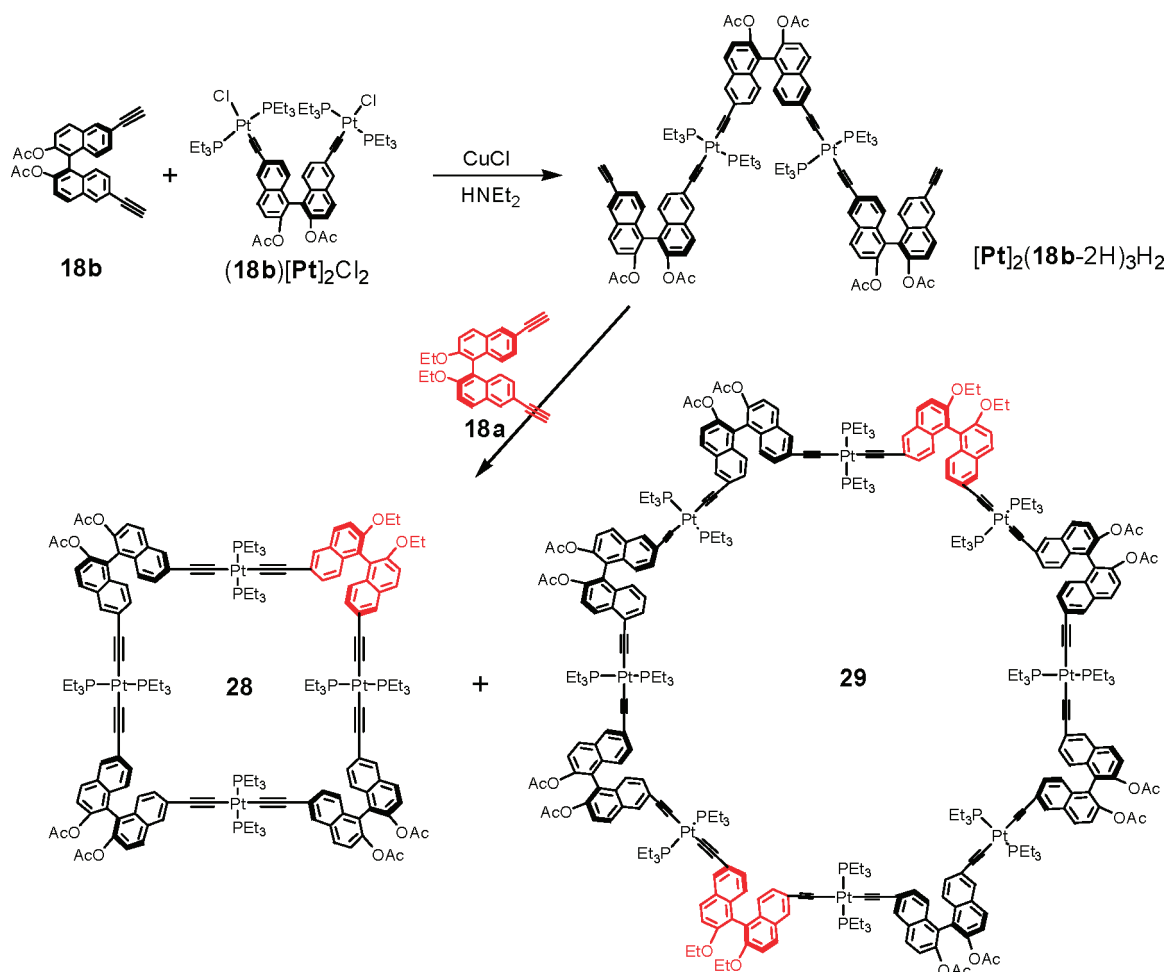
FIGURE 17. Synthesis of homochiral metallocycles containing bridging ligands with different protecting groups.

of **18b**/**18a** = 3:1. The two ligands **18a** are separated by three ligands **18b** in the octagon, which results in D_2 symmetry. The acetyl protecting groups in the metallocycles were readily removed by treating with inorganic bases to give hydroxyl-containing metallocycles.[38] For example, the molecular square [*trans*-(PEt₃)₂Pt(**18b**)]₄ was treated with K_2CO_3 in MeOH and THF to afford metallocycle [*trans*-(PEt₃)₂Pt(**18**-OH)]₄ with hydroxyl functional groups, which was further converted to new metallocycles with other functionalities, such as octadecyl chains or Frechét dendrons.

All of the Pt–alkynyl metallocycles described above were built from enantiopure bridging ligands of the same handedness. The directed-assembly approach was also used to introduce ligands of the opposite chirality to generate non-homochiral metallocycles.[21] The oligomers (*R,S,R*)-[Pt]₂(**18b**)₃H₂ and (*R,S,R,S,R*)-[Pt]₄(**18b**)₅H₂ were prepared by treating (*R*)-**L**-H₂ with 0.25 equiv of [(*S*)-**18b**][Pt]₂Cl₂ at 0 °C in the presence of a CuCl catalyst (Figure 18). Molecular square (*R,S,R,S*)-[*trans*-(PEt₃)₂-Pt(**18b**)]₄ and octagon (*R,S,R,S,R,S,R,S*)-[*trans*-(PEt₃)₂Pt(**18b**)]₈ were obtained in high yields (76% and

8%, respectively) by treating (*R,S,R*)-[Pt]₂(**18b**-2H)₃H₂ with 1 equiv of [(*S*)-**18b**][Pt]₂Cl₂ at room temperature in the presence of a catalytic amount of CuCl. Molecular square (*R,R,R,S*)-[*trans*-(PEt₃)₂Pt(**18b**)]₄ and octagon (*R,R,R,S,R,R,R,S*)-[*trans*-(PEt₃)₂Pt(**18b**)]₈ were prepared in 83% and 10% yield, respectively, by treating (*R,R,R*)-[Pt]₂(**18b**)₃H₂ with 1 equiv of [(*S*)-**18b**][Pt]₂Cl₂ at room temperature in the presence of a catalytic amount of CuCl. Molecular square (*R,R,S,S*)-[*trans*-(PEt₃)₂Pt(**18b**)]₄ and octagon (*R,R,S,S,R,R,S,S*)-[*trans*-(PEt₃)₂Pt(**18b**)]₈ were prepared in 76% and 12% yield, respectively, by treating (*R,R*)-(**18b**)₂[Pt]₃Cl₂ with 1 equiv of (*S,S*)-[Pt](**18b**)₂H₂. The present synthetic approach thus allows the synthesis of all of four diastereomeric molecular squares by simply starting from building blocks of desired chirality. The non-homochiral molecular squares and octagons were characterized by ¹H{³¹P}, ³¹P{¹H}, and ¹³C{¹H} NMR spectroscopy and MALDI-TOF MS. The ¹H{³¹P}, ³¹P{¹H}, and ¹³C{¹H} NMR spectra of molecular square (*R,S,R,S*)-[*trans*-(PEt₃)₂Pt(**18b**)]₄ and octagon (*R,S,R,S,R,S,R,S*)-[*trans*-(PEt₃)₂Pt(**18b**)]₈ show a single ligand environment due to the same chemical environments
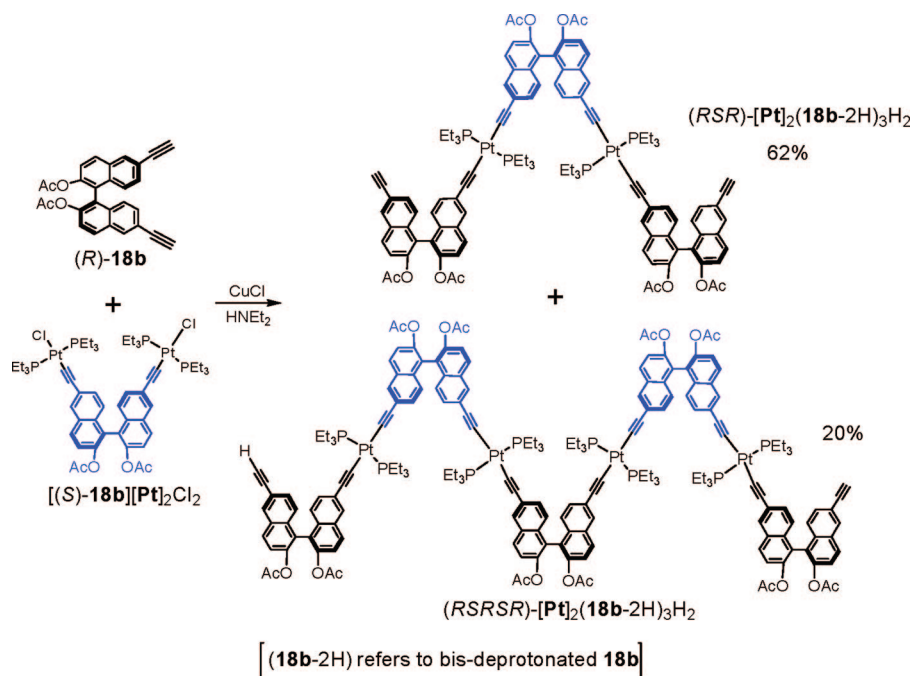
FIGURE 18. Synthesis of building units for non-homochiral metallocycles.

of both (*R*)- and (*S*)-bridging ligands, which is consistent with D_{2d} symmetry of the square and D_{4d} symmetry of the octagon. In contrast, the $^1H\{^{31}P\}$ and $^{31}P\{^1H\}$ NMR spectra of the molecular square (*R,R,S,S*)-[*trans*-(PEt$_3$)$_2$Pt(**18b**)]$_4$ and octagon (*R,R,S,S,R,R,S*)-[*trans*-(PEt$_3$)$_2$Pt(**18b**)]$_8$ show two sets of peaks, corresponding to two different chemical environments for the naphthyl groups and [Pt] centers, corresponding to C_{2h} symmetry of the square and D_{2d} symmetry of the octagon. The $^1H\{^{31}P\}$ NMR spectra of the molecular square (*R,R,R,S*)-[*trans*-(PEt$_3$)$_2$Pt(**18b**)]$_4$ and octagon (*R,R,R,S,R,R,R,S*)-[*trans*-(PEt$_3$)$_2$-Pt(**18b**)]$_8$ show broad peaks due to the overlap of signals from the naphthyl groups in four different chemical environments. The retention times of the non-homochiral squares and octagons are a little larger than those of the corresponding homochiral squares and octagons, which indicate smaller sizes of non-homochiral cycles. This is because the non-homochiral cycles adopt butterfly structures rather than the more planar geometry seen in the homochiral metallocycles (Figure 19).

Chiral Metallocycles as Luminescent Materials in Light-Emitting Devices

Compound **17** was explored for application in a light-emitting device by taking advantage of an interesting luminescence property of the Pt(diimine) moieties.[39−41] The thin film of **17** shows significantly red-shifted and broadened emissions at ~730 nm, suggesting its severe aggregation in thin films (Figure 20a).[33] Weak fluorescence peaks at ~440 nm observed in a solution of **17** completely disappeared. Consis-

tent with the aggregation behavior of **17**, LED devices with structure ITO/PEDOT−PSS/EL layer/CsF/Al, where PEDOT−PSS denotes poly(ethylene dioxythiophene) doped with poly(styrene sulfonate) and EL layer is **17**, gave very broad emissions at ~730 nm with highest brightness of only <20 cd m^{-2} (Figure 20b). The poor device performance is presumably a result of aggregation quenching of triplet emissions. To alleviate aggregation quenching, **17** was doped into poly(*N*-vinylcarbazole) (PVK), a well-known hole-transport polymer. The PL spectra of spin-coated films of the blends of **17** and PVK showed significant blue shift of the triplet emissions of **17** (Figure 20a). It is also evident from Figure 20a that energy transfer between PVK and **17** is rather inefficient. Interestingly, the EL spectra of **17** in a similar device structure showed mostly triplet emission of **17** at longer wavelength (Figure 20b), consistent with a dominant direct charge-trapping mechanism (instead of intermolecular energy transfer) in the EL process. Very bright and efficient LEDs were built based on the blends of **17** and PVK. For the blend with 5 wt % **17** in PVK, the maximum brightness reaches 5470 cd m^{-2} with a maximum luminous efficiency of 0.93 cd A^{-1}. This level of performance is superior to that reported for simple bis(acetylide)Pt(II) complexes.

Chiral Metallocycles for Enantioselective Sensing and Asymmetric Catalysis

Due to their outstanding asymmetric discrimination and stable chiral configuration, the metallocycle **6d** shows interest-
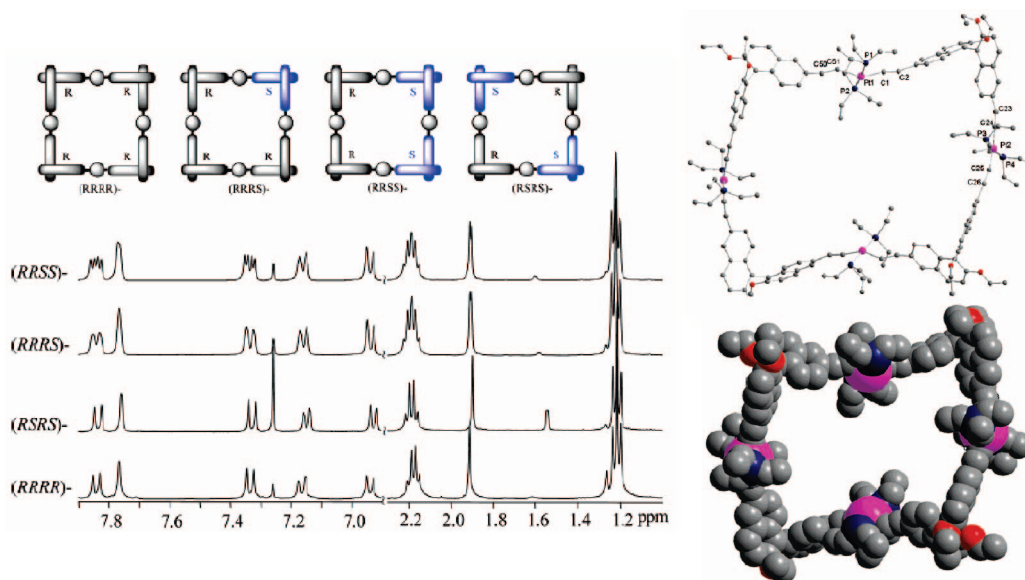
FIGURE 19. $^1H\{^{31}P\}$ NMR spectra of non-homochiral and homochiral squares [*trans*-$(PEt_3)_2Pt(\textbf{18b})]_4$ and single-crystal X-ray structure (right top) and a space-filling model (right bottom) of (R,S,R,S)-[*trans*-$(PEt_3)_2Pt(\textbf{18a})]_4$.
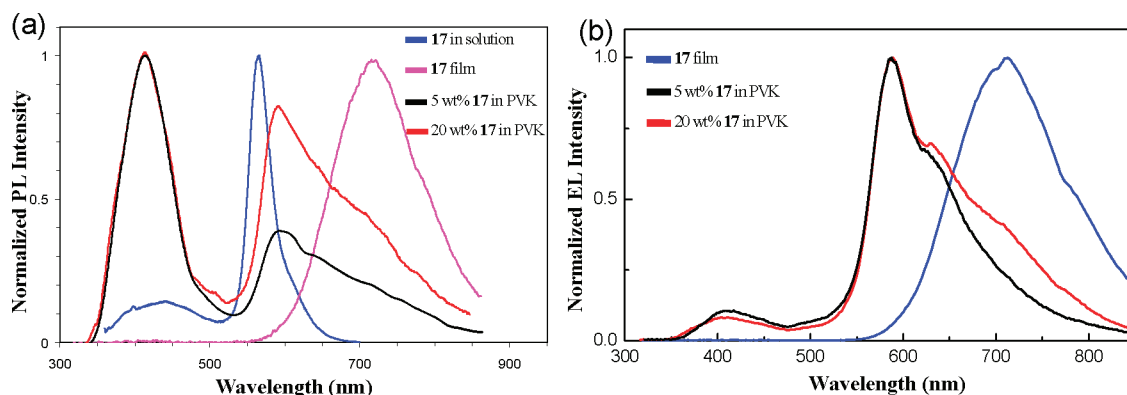

FIGURE 20. PL (a) and EL (b) of **17** in solution, thin film, and PVK blends.

ing enantioselective luminescence quenching behavior by chiral amino alcohols in THF.[29] The luminescence signal of enantiopure (R)-**6d** at 412 nm can be quenched by both enantiomers of 2-amino-1-propanol but at significantly different rates. Figure 21 shows the Stern–Völmer plots of (R)-**6d** (2.2 $\times$ 10^{-6} M) in the presence of (R)- and (S)-2-amino-1-propanol in THF. It is evident that luminescence quenching of chiral metallocycle **6d** by 2-amino-1-propanol is enantioselective. For (R)-**6d**, the Stern–Völmer quenching constant K_{sv} is 7.35 M^{-1} in the presence of (S)-2-amino-1-propanol, and 6.02 M^{-1} in the presence of (R)-2-amino-1-propanol. (R)-**6d** has an enantioselectivity factor $k_{sv}(R-S)/k_{sv}(R-R)$ of 1.22 for luminescence quenching in favor of (S)-2-amino-1-propanol. The opposite trend in enantioselectivity was observed for the quenching of (S)-**6d** by 2-amino-1-propanol, which lends further support to a chirality-based luminescence-quenching selectivity. This magnitude of enantioselectivity for **6d** is significantly higher
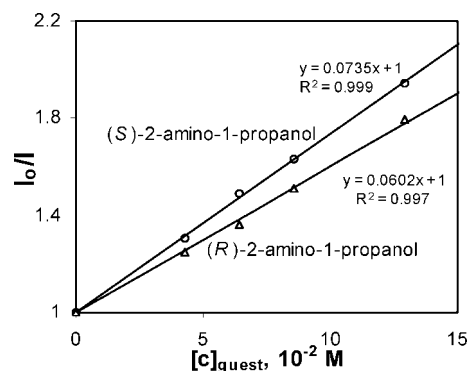
FIGURE 21. Stern–Völmer plots of (R)-**6d** (2.2 $\times$ 10^{-6} M) in the presence of (S)- and (R)-2-amino-1-propanol.

that of free ligand **5d**, which shows an enantioselective factor of 1.04, suggesting a better-defined chiral environment conferred by metallocycle **6d**. It has been proposed that the formation of a nonemissive hydrogen-bonded complex and a poorly emissive excited-state proton-transfer complex is

TABLE 2. Diethylzinc Additions to Aldehydes Catalyzed by Ti(IV) Complexes of **10d**

$$Ar \overset{O}{\underset{H}{\diagdown}} + Et_2Zn \xrightarrow[\text{Ti(O}^i\text{Pr)}_4]{(S)\text{-}\textbf{10d}} Ar \overset{HO\ \ H}{\underset{Et}{\diagdown}} \qquad (\text{Eq. 1})$$

Entry	Aldehyde	Temp	Conversion	e.e.
1		rt	>95%	91
2		rt	>95%	91
		0 °C	>95%	92
3		rt	>95%	90
4		rt	>95%	91
5		rt	>95%	89
6		rt	>95%	90

TABLE 3. Diethylzinc Additions to Aldehydes Catalyzed by Ti(IV) Complexes of **19c** at 0 °C

Aldehyde	Time (h)	Conversion	e.e. (%)
	16	>95%	84
	16	>95%	94
	16	>95%	78
	40	~40%	78
	40	~80%	77
	16	>95%	78

responsible for the luminescence quenching of phenylene-acetylene dendrimers with BINOL core by amino alcohols.[42] It is interesting to note that no enantioselectivity was observed for the luminescence quenching of **6d** by 1-amino-2-propanol, which supports the involvement of amino groups in the formation of a ground-state hydrogen-bonded complex and an excited-state proton transfer complex.[43]

Molecular triangle **10d** contains chiral dihydroxy functionalities and was used for highly enantioselective catalytic diethylzinc additions to aromatic aldehydes, which afforded chiral secondary alcohols upon hydrolytic workup as shown in eq 1.[31] With Ti(IV) complexes of **10d** as the catalyst, chiral secondary alcohols were obtained in greater than 95% yield and 89−92% ee for a wide range of aromatic aldehydes with varying steric demands and electronic properties (Table 2). In comparison, when the free ligand 6,6′-dichloro-4,4′-diethynyl-2,2′-binaphthol was used instead of **10d**, a lower ee (80%) was obtained for the addition of diethylzinc to 1-naphthaldehyde. The broad substrate scope for catalytic diethylzinc additions using **10d** and Ti(O^{i}Pr)$_4$ suggests that there is significant flexibility in the dihydroxy groups to accommodate aldehydes of various sizes.

As shown in Table 3, the Ti(IV) complexes of **19c** are excellent catalysts for the additions of diethylzinc to 1-naphthaldehyde with 94% ee and >95% conversion at 0 °C.[34] The enantioselectivity has however dropped significantly when other smaller aromatic aldehydes were used as the substrates. This result differs from the performance of **10d**, which has a very broad substrate scope. Such a difference is believed to be a direct consequence of much more rigid structure of **19c**; the dihedral angles of naphthyl rings in the Ti(IV) catalyst cannot vary to accommodate aldehydes of various sizes to give high

enantioselectivity. The chiral dihydroxy groups in **19c** thus differ from those of BINOL and may prove useful for mechanistic work owing to their rigid structure.

Interestingly, the steric congestion around the chiral dihydroxy groups in isomeric metallacyclophane **21c** prevented its reaction with Ti(O^{i}Pr)$_4$ to form active catalysts for diethylzinc additions to aromatic aldehydes. This result highlights the influence of supramolecular arrangement on not only stereoselectivity but also activity of asymmetric catalysts derived from metallocycles.

Allosteric Regulation of Chiral Metallocycles

Chiral metallocycles synthesized via the weak-link approach (WLA) can exhibit significant changes in the size and shape of the macrocyclic cavities upon the introduction of other ligands.[44] Mirkin and co-workers have recently demonstrated novel allosteric effects on the metallocycles built using the weak-link approach (WLA).[45] When an allosteric effector is introduced to the condensed intermediate templated by hemilabile ligands, it can strategically form both strong and weak coordination bonds with metal centers to selectively and reversibly open the condensed intermediate into a flexible macrocycle.[45−47] For example, the metallocycle **31** containing two structural domains (Rh(I)) and two catalytic domains (Zn(II)) can be opened to form **32** by the introduction of CO gas (1 atm) in the presence of Cl$^-$ ions in CH$_2$Cl$_2$ (Figure 21).[48] Both CO and Cl$^-$ are required to break the thioether/Rh(I) bonds, leaving the phosphine/Rh(I) bonds intact. The result of the selective breaking of these bonds is a concomitant significant change in molecular shape. This opened cavity allows substrate molecules to enter, where they undergo a fast intramolecular reaction. Since the acyl transfer reaction between acetic anhydride and pyridyl carbinol
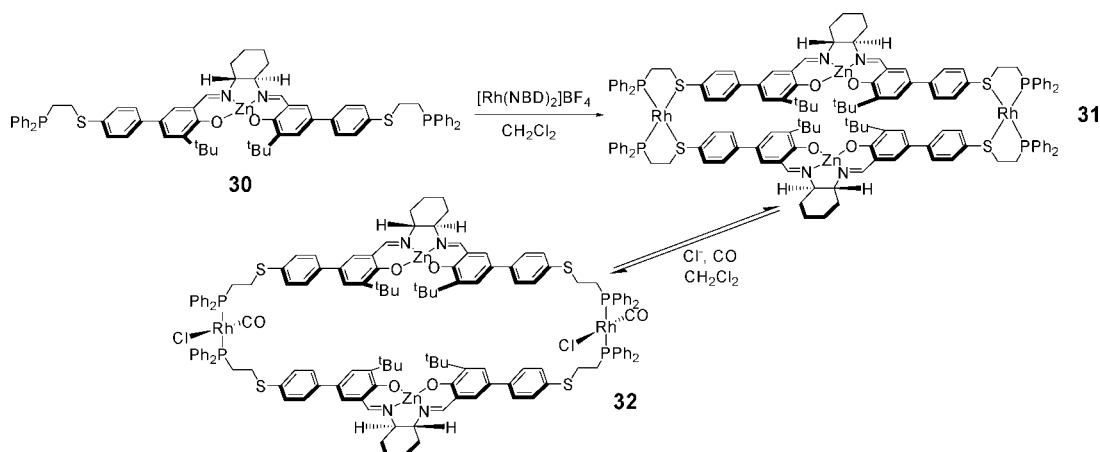
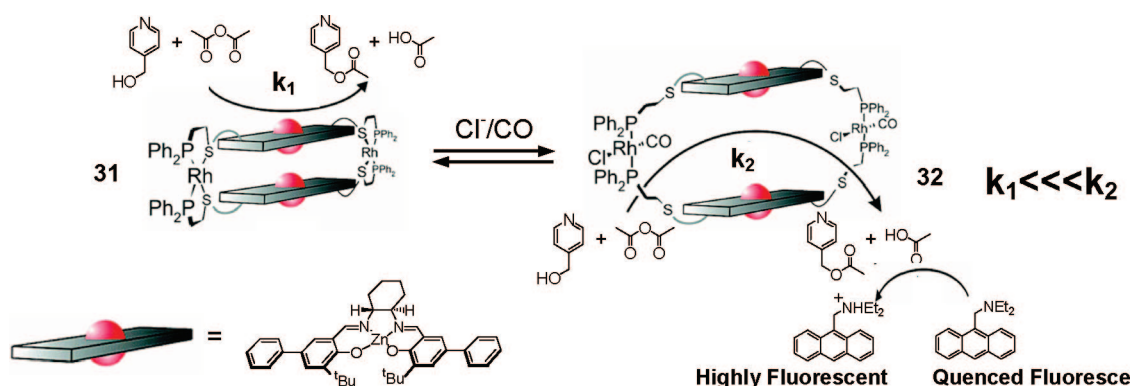**FIGURE 22.** Synthesis of allosteric chiral metallocycles.

FIGURE 23. Analyte binding opens the cavity and allows substrate molecules to enter, where they undergo a fast intramolecular reaction to generate acetic acid, which protonates a pH-sensitive fluorescent probe.
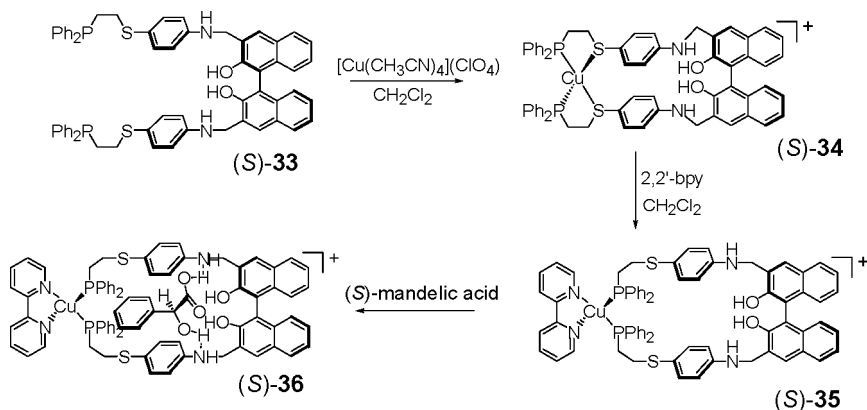

FIGURE 24. Synthesis of allosteric chiral metallocycles (*S*)-**34** and (*S*)-**35** and mandelic acid complexed metallocycle (*S*)-**36**.

can be catalyzed in a bimetallic fashion, this allosteric catalyst increases the reaction rate significantly (Figure 22). The incorporation of a pH-sensitive fluorophore (diethylaminomethylanthracene) to interact with the reaction byproduct, acetic acid, provides a straightforward method for visually and spectrophotometrically monitoring the reaction (Figure 23).

Allosteric metallocycles were recently employed in enantioselective recognition of chiral mandelic acid.[49] Enantiomerically pure (*S*)-**33** was treated with 1 equiv of [Cu(CH$_3$CN)$_4$](ClO$_4$) in CH$_2$Cl$_2$ to form the condensed intermediate (*S*)-**34**, which was further reacted with 2,2'-bpy (1 equiv) in CH$_2$Cl$_2$ to yield an opened structure (*S*)-**35** (Figure 24). When closed complex (*S*)-**34** was treated with a large

excess of (*S*)- or (*R*)-mandelic acid, no significant changes in the fluorescence intensities were observed, which is because the binding pocket is closed and the multiple hydrogen-bonding sites required to complex mandelic acid are not accessible. However, open complex (*S*)-**35** can accommodate mandelic acid, and the fluorescence intensity of (*S*)-**35** increases in the presence of (*S*)- or (*R*)- mandelic acid. This increase in fluorescence is due to the suppressed photoinduced electron-transfer fluorescence quenching as the amine nitrogen atom of (*S*)-**35** is protonated by the acid. In solution with CH_2Cl_2 (containing 2% 1,2-dimethoxyethane (DME)), the fluorescence intensity of (*S*)-**35** (1.0×10^{-4} M) was increased 3.1-fold upon treatment with (*S*)-mandelic acid (5.0×10^{-3} M) but only 1.9-fold with (*R*)-mandelic acid (5.0×10^{-3} M). The net fluorescence intensity increase of (*S*)-**35** by (*S*)-mandelic acid was 2.33 times that by (*R*)-mandelic acid.

Summary and Outlook

Significant progress has been made on the rational design of chiral metallocycles over the past decade. Numerous chiral metallocycles ranging from dimeric metallacyclophanes to unprecedentedly large metallocycles with 47 metallocorners were synthesized with three distinct synthetic strategies. Unlike their covalent organic counterparts, chiral metallocycles can be constructed with unprecedented predictability and ease via judicious choices of multitopic bridging ligands and unsaturated metal centers. The newly developed directed-assembly routes allow the synthesis of chiral metallocycles with much enhanced stability, favorable solubility charactersitics, unprecedentedly large sizes, well-positioned functional groups, and desired chirality. The applications of these chiral metallocycles in light-emitting devices, allosteric regulation, chiral sensing, and asymmetric catalysis have been demonstrated. The influences of supramolecular arrangement on chiral molecular sensing and both activity and stereoselectivity of asymmetric catalysts derived from metallocycles were established. The examples illustrated in this Account give testimony to chemists' ability, through chemical manipulations, to create large and complex chiral metallocycles that can potentially serve as mimics of natural enzyme systems, from sensing to catalysis. Future advances in this area will likely be directed toward further exploitation of supramolecular functions of chiral metallocycles in many applications, including molecular recognition, host−guest interaction, chiral recognition, and catalysis. Such research efforts will lead to new materials with desirable and tunable properties and ultimately to the demonstration of nanoscale devices and molecular machinery.

BIOGRAPHICAL INFORMATION

Suk Joong Lee received his B.S. and M.S. degrees from Yonsei University, Korea and Ph.D. degree from the University of North Carolina at Chapel Hill. He is currently a postdoctoral fellow in the department of chemistry at Northwestern University.

Wenbin Lin is Professor of Chemistry and Pharmacy at the University of North Carolina at Chapel Hill. His research focuses on crystal engineering of functional solids, rational synthesis of chiral supramolecular systems, designing metallopharmaceuticals for cancer imaging and therapy, and developing hybrid nanomaterials for biological and biomedical applications.

REFERENCES

1 Fujita, M.; Ogura, K. Transition-Metal-Directed Assembly of Well-Defined Organic Architectures Possessing Large Voids: From Macrocycles to [2]Catenanes. *Coord. Chem. Rev.* **1996**, *148*, 249–264.

2 Fujita, M. Metal-Directed Self-Assembly of Two- and Three-Dimentional Synthetic Receptors. *Chem. Soc. Rev.* **1998**, *27*, 417–425.

3 Stoddard, J. F., Ed. *Monographs in Supramolecular Chemistry*; Royal Society of Chemistry: Cambridge, U.K., 1991.

4 Lehn, J.-M., Chair, Ed., Chair Ed.; Atwood, J. L.; Davis, J. E. D.; MacNicol, D. D., Vögtle, F. Exec. Eds. *Comprehensive Supramolecular Chemistry*; Pergamon: Oxford, U.K., 1987–1996, Vols. 1–11.

5 Leininger, S.; Olenyuk, B.; Stang, P. J. Self-Assembly of Discrete Cyclic Nanostructures Mediated by Transition Metals. *Chem. Rev.* **2000**, *100*, 853–908.

6 Wu, A.; Isaacs, L. Self-Sorting: The Exception or the Rule. *J. Am. Chem. Soc.* **2003**, *125*, 4831–4835.

7 Stang, P. J.; Olenyuk, B. Self-Assembly, Symmetry, and Molecular Architecture: Coordination as the Motif in the Rational Design of Supramolecular Metallocyclic Polygons and Polyhedra. *Acc. Chem. Res.* **1997**, *30*, 502–518.

8 Shimizu, K. D.; Rebek, J., Jr. Synthesis and Assembly of Self-Complementary Calix[4]arenes. *Proc. Natl. Acad. Sci. U.S.A.* **1995**, *92* (26), 12403–12407.

9 Lawrence, D. S.; Jiang, T.; Levett, M. Self-Assembling Supramolecular Complexes. *Chem. Rev.* **1995**, *95*, 2229–2260.

10 Whitesides, G. M.; Simanek, E. E.; Methias, J. P.; Seto, C. T.; Chin, D.; Mammen, M.; Gordon, D. M. Noncovalent Synthesis: Using Physical-Organic Chemistry To Make Aggregates. *Acc. Chem. Res.* **1995**, *28*, 37–44.

11 Hasenknopf, B.; Lehn, J.-M.; Boumediene, N.; Dupont-Gervais, A.; Dorsselaer, A. V.; Kneisel, B.; Fenske, D. Self-Assembly of Tetra- and Hexanuclear Circular Helicates. *J. Am. Chem. Soc.* **1997**, *119*, 10956–10962.

12 Aoyagi, M.; Biradha, K.; Fujita, M. Quantitative Formation of Coordination Nanotubes Templated by Rodlike Guests. *J. Am. Chem. Soc.* **1999**, *121*, 7457–7458.

13 Olenyuk, B.; Whiteford, J. A.; Fechtenkötter, A.; Stang, P. J. Self-Assembly of Nanoscale Cuboctahedra by Coordination Chemistry. *Nature* **1999**, *398*, 796–799.

14 Sato, S.; Iida, J.; Suzuki, K.; Kawano, M.; Ozeki, T.; Fujita, M. Fluorous Nanodroplets Structurally Confined in an Organopalladium Sphere. *Science* **2006**, *313*, 1273– 1276.

15 Olenyuk, B.; Fechtenköter, A.; Stang, P. J. Molecular Architecture of Cyclic Nanostructures: Use of Coordination Chemistry in the Building of Supermolecules with Predefined Geometric Shapes. *J. Chem. Soc., Dalton Trans.* **1998**, 1707–1728.

16 Chi, X.; Guerin, A. J.; Haycock, R. A.; Hunter, C. A.; Sarson, L. D. The Thermo-dynamics of Self-Assembly. *J. Chem. Soc., Chem. Commun.* **1995**, 2563–2565.

17 Chi, X.; Guerin, A. J.; Haycock, R. A.; Hunter, C. A.; Sarson, L. D. Self-Assembly of Macrocyclic Porphyrin Oligomers. *J. Chem. Soc., Chem. Commun.* **1995**, 2567– 2569.

18 Fujita, M.; Sasaki, O.; Mitsuhashi, T.; Fujita, T.; Yazaki, J.; Yamaguchi, K.; Ogura, K. On the Structure of Transition-Metal-Linked Molecular Squares. *J. Chem. Soc., Chem. Commun.* **1996**, 1535–1536.

19 Lee, S. B.; Hwang, S. G.; Chung, D. S.; Yun, H.; Hong, J.-I. Guest-Induced Reorganization of a Self-Assembled Pd(II) Complex. *Tetrahedron Lett.* **1998**, *39*, 873–876.

20 Lee, S. J.; Hupp, J. T. Porphyrin-Containing Molecular Squares: Design and Applications. *Coord. Chem. Rev.* **2006**, *250*, 1710–1723.

21 Jiang, H.; Lin, W. Directed Assembly of Mesoscopic Metallocycles with Controllable Size, Chirality, and Functionality Based on the Robust Pt-Alkynyl Linkage. *J. Am. Chem. Soc.* **2006**, *128*, 11286–11297.

22 Noyori, R. Asymmetric Catalysis: Science and Opportunities (Nobel Lecture). *Angew. Chem., Int. Ed.* **2002**, *41*, 2008–2022.

23 Patel, R. N., Ed. *Stereoselective Biocatalysis*; Marcel Dekker: New York, 1999.

24 Lee, S. J.; Lin, W. Chiral Macrocycles. In *Encyclopedia of Nanoscience and Nanotechnology*; Nalwa, H. S., Ed.; American Scientific: Stevenson Ranch, U.S.A. 2003; Vol 1, pp 863–875.

25 Oenyuk, B.; Whiteford, J. A.; Stang, P. J. Design and Study of Synthetic Chiral Nanoscopic Assemblies. Preparation and Characterization of Optically Active Hybrid, Iodonium-Transition-Metal and All-Transition-Metal Macrocyclic Molecular Squares. *J. Am. Chem. Soc.* **1996**, *118*, 8221–8230.

26 Fan, J.; Whitehold, J. A.; Olenyuk, B.; Levin, M. D.; Stang, P. J.; Fleischer, E. B. Self-Assembly of Porphyrin Arrays via Coordination to Transition Metal Bisphosphine Complexes and the Unique Spectral Properties of the Product Metallacyclic Ensembles. *J. Am. Chem. Soc.* **1999**, *121*, 2741–2752.

27 Zhang, Y.; Wang, S.; Enright, G. D.; Breeze, S. R. Tetraacetylethane Dianion (Tae) As a Bridging Ligand for Molecular Square Complexes: $Co^{II}_4(Tae)_4(Dpa)_4$, Dpa = Di-2-pyridylamine, a Chiral Molecular Square in the Solid State. *J. Am. Chem. Soc.* **1998**, *120*, 9398–9399.

28 Ali, M. M.; MacDonnell, F. M. Topospecific Self-Assembly of Mixed-Metal Molecular Hexagons with Diameters of 5.5 nm Using Chiral Control. *J. Am. Chem. Soc.* **2000**, *122*, 11527–11528.

29 Lee, S. J.; Lin, W. A Chiral Molecular Square with Metallo-Corners for Enantioselective Sensing. *J. Am. Chem. Soc.* **2002**, *124*, 4554–4555.

30 Lee, S. J.; Kim, J. S.; Lin, W. Chiral Molecular Squares Based on Angular Bipyridines: Self-Assembly, Characterization, and Photophysical Properties. *Inorg. Chem.* **2004**, *43*, 6579–6588.

31 Lee, S. J.; Hu, A.; Lin, W. The First Chiral Organometallic Triangle for Asymmetric Catalysis. *J. Am. Chem. Soc.* **2002**, *124*, 12948–12949.

32 Lee, S. J.; Luman, C. R.; Castellano, F. N.; Lin, W. Directed Assembly of Chiral Organometallic Squares that Exhibit Dual Luminescence. *Chem. Commun.* **2003**, *17*, 2124–2125.

33 Zhang, L.; Niu, Y.-H.; Jen, A. K.-Y.; Lin, W. A Highly Electroluminescent Molecular Square. *Chem. Commun.* **2005**, 1002–1004.

34 Jiang, H.; Hu, A.; Lin, W. A Chiral Metallacyclophane for Asymmetric Catalysis. *Chem. Commun.* **2003**, 96–97.

35 Jiang, H.; Lin, W. Chiral Metallacyclophanes: Self-Assembly, Characterization, and Application in Asymmetric Catalysis. *Org. Lett.* **2004**, *6*, 861–864.

36 Jiang, H.; Lin, W. Self-Assembly of Chiral Molecular Polygons. *J. Am. Chem. Soc.* **2003**, *125*, 8084–8085.

37 Jiang, H.; Lin, W. Expeditious Assembly of Mesoscopic Metallocycles. *J. Am. Chem. Soc.* **2004**, *126*, 7426–7427.

38 Jiang, H.; Lin, W. Chiral Molecular Polygons Based on the Pt-Alkynyl Linkage: Self-Assembly, Characterization, and Functionalization. *J. Organomet. Chem.* **2005**, *690*, 5159–5169.

39 Chan, C.-W.; Cheng, L.-K.; Che, C.-M. Luminescent Donor-Acceptor Platinum(II) Complexes. *Coord. Chem. Rev.* **1994**, *132*, 87–97.

40 McGarrah, J. E.; Eisenberg, R. Dyads for Photoinduced Charge Separation Based on Platinum Diimine Bis(acetylide) Chromophores: Synthesis, Luminescence and Transient Absorption Studies. *Inorg. Chem.* **2003**, *42*, 4355–4365.

41 Chan, S.-C.; Chan, M. C. W.; Wang, Y.; Che, C.-M.; Cheung, K.-K.; Zhu, N. Organic Light-Emitting Materials Based on Bis(arylacetylide)platinum(II) Complexes Bearing Substituted Bipyridine and Phenanthroline Ligands: Photo- and Electroluminescence from ^{3}MLCT Excited States. *Chem.—Eur. J.* **2001**, *7*, 4180–4190.

42 Pugh, V. J.; Hu, Q.-S.; Pu, L. The First Dendrimer-Based Enantioselective Fluorescent Sensor for the Recognition of Chiral Amino Alcohols. *Angew. Chem., Int. Ed.* **2000**, *39*, 3638–3641.

43 Pugh, V. J.; Hu, Q.-S.; Zuo, X.; Lewis, F. D.; Pu, L. Optically Active BINOL Core-Based Phenyleneethynylene Dendrimers for the Enantioselective Fluorescent Recognition of Amino Alcohols. *J. Org. Chem.* **2001**, *66*, 6136–6140.

44 Gianneschi, N. C.; Masar, M. S.; Mirkin, C. A. Development of a Coordination Chemistry-Based Approach for Functional Supramolecular Structures. *Acc. Chem. Res.* **2005**, *38*, 825–837.

45 Masar, M. S.; Gianneschi, N. C.; Oliveri, C. G.; Stern, C. L.; Nguyen, S. T.; Mirkin, C. A. Allosterically Regulated Supramolecular Catalysis of Acyl Transfer Reactions for Signal Amplification and Detection of Small Molecules. *J. Am. Chem. Soc.* **2007**, *129*, 10149–10158.

46 Eisenberg, A. H.; Ovchinnikov, M. V.; Mirkin, C. A. Stepwise Formation of Heterobimetallic Macrocycles Synthesized via the Weak-Link Approach. *J. Am. Chem. Soc.* **2003**, *125*, 2836–2837.

47 Khoshbin, M. S.; Ovchinnikov, M. V.; Mirkin, C. A.; Zakharov, L. N.; Rheingold, A. L. Binuclear Ruthenium Macrocycles Formed via the Weak-Link Approach. *Inorg. Chem.* **2005**, *44*, 496–501.

48 Gianneschi, N. C.; Nguyen, S. T.; Mirkin, C. A. Signal Amplification and Detection via a Supramolecular Allosteric Catalyst. *J. Am. Chem. Soc.* **2005**, *127*, 1644–1645.

49 Heo, J.; Mirkin, C. A. Pseudo-Allosteric Recognition of Mandelic Acid with an Enantioselective Coordination Complex. *Angew. Chem., Int. Ed.* **2006**, *45*, 941–944.